BOUNDARY-LAYER ANALYSIS OF HEAT AND MASS TRANSFER OVER A CIRCULAR CYLINDER IN CROSSFLOW

Byung Kyu KIM

Department of Chemical Engineering, University of Ulsan, Ulsan 690, Korea

(Received 12 May 1986 • accepted 21 October 1986)

Abstract — Two-dimensional laminar boundary-layer equations of momentum, heat and mass transfer have been numerically solved under forced convection. A finite difference approximation of the governing equations in a Goertler-type variable domain has been implemented on computer. To provide rigorous initial conditions at x = 0 in the boundary-layer code, differential equations governing heat and mass transfer in the stagnation region have been set up and solved numerically.

The effect of outer flow condition on skin friction as well as heat and mass transfer has been demonstrated. Results obtained made an improvement over past theoretical predictions based on analytical approximation, and agreed favorably with experimental data available.

INTRODUCTION

Momentum, heat and mass transfer around a circular cylinder in crossflow has long been a popular topic for both theoretical and experimental investigators. This, perhaps, is due to the industrial significance of this relatively simple geometry-flow system oftentimes encountered like in heat exchanger, packing tower, catalytic reactor designs etc.. The advance of this area of study has well been balanced between theoretical and experimental parts of studies, and a number of valuable review papers became available in the past. These include a fair comparative study of experimental investigations up to 1948 by Winding and Cheney [1], an exhaustive review over fifteen prediction methods up to 1962 by Spalding and Pun [2], and a comprehensive review over two hundred experimental and theoretical works up to 1972 by Zukauskas [3].

The present study is confined to a theoretical prediction of heat and mass transfer from a circular cylinder in laminar crossflow under forced convection. Earlier theoretical predictions will only be briefly mentioned here as they relate to the present investigations. The task in this area was to solve the laminar boundary-layer equations of continuity, motion, thermal energy, and the continuity of diffusant. Solution methods to the two-dimensional (2-D) boundary-layer equations so far reported were limited to the analytical approximation except the one by Frössling [4] who solved the boundary-layer equations by a series method which in nature is exact. However, the accuracy of this method

was also limited practically by the number of terms available in series expansion. The solution thereupon obtained is regarded an exact only near the front stagnation point. Other useful methods of solution are essentially based on similarity solutions which are exact as far as the boundary layers are similar. The boundary layer around the circular cylinder in crossflow is only locally similar and therefore the similarity solution involves certain level of inaccuracy in general. The majority of the prediction methods are contained in Ref. (2), and the readers are referred to this paper for further details. Several methods of prediction were also reported later, however, these are essentially analytical approximations based on similarity solution [5 and 6]. Exact numerical solutions to the boundary-layer equations were provided by Krall and Eckert [7] using the method of finite difference. Constant wall temperature and constant heat flux boundary conditions were both considered in this paper. The validity of this exact solution was however confined to the low Reynolds number flows certainly excluding the separation characteristics.

In the present investigation a finite difference method has been employed to provide exact numerical solutions to the 2-D laminar boundary-layer equations under forced convection. The method of finite difference, of course, today is a fairly simple exercise. However, to the knowledge of present author no one has attempted to solve the problem by this method in practical Reynolds number range, and it should be more reliable than any other asymptotic methods.

MATHEMATICAL MODELING

The governing equations of momentum, heat and mass transfer of 2-D laminar boundary-layer flows are formulated in this section. A forced convection with no viscous dissipation has been assumed. The mass transfer problem is limited to convective transport of a nonreacting binary system of dilute solution, which still has ample applications [8].

Governing equations

The dimensional form of the governing equations in terms of conventional notation for the flow of an incompressible continuum in two dimensions (see the coordinate system in Fig. 1) reads

$$\frac{\partial u}{\partial x} - \frac{\partial v}{\partial y} = 0 \tag{1}$$

$$u\frac{\partial u}{\partial x} + v\frac{\partial u}{\partial y} - U\frac{\partial U}{\partial x} = \nu\frac{\partial^2 u}{\partial y^2} \tag{2}$$

$$u\frac{\partial T}{\partial x} + v\frac{\partial T}{\partial y} = \alpha\left(\frac{\partial^2 T}{\partial x^2} + \frac{\partial^2 T}{\partial y^2}\right) \tag{3}$$

$$u\frac{\partial C}{\partial x} + v\frac{\partial C}{\partial y} = D\left(\frac{\partial^2 C}{\partial x^2} + \frac{\partial^2 C}{\partial y^2}\right) \tag{4}$$

The initial and boundary conditions considered are:

$$u(x, 0) = v(x, 0) = 0 \tag{5}$$
$$T(x, 0) = T_w \tag{6}$$
$$C(x, 0) = C_w \tag{7}$$
$$u(x, \infty) = U(x) \tag{8}$$
$$T(x, \infty) = T_e \tag{9}$$
$$C(x, \infty) = C_e \tag{10}$$

In the above, U is the outer flow velocity distribution, that is the inner limit of the outer expansion, and ν, α and D are the kinematic viscosity, thermal diffusivity and binary diffusivity, respectively. Equation (5) dic-

Fig. 1. Boundary-layer coordinate.

tates no slip, no penetration at the wall, eqs. (6) and (7) superpose constant wall temperature and constant wall concentration conditions, and the conditions at the boundary-layer edges are defined by eqs. (8)-(10). To sweep the 2-D boundary layer, conditions at x = 0 plane should be imposed. This will be discussed at the end of this section.

Nondimensionalization and boundary-layer approximation

The dimensionless variables are defined by

$$x^* = x/L, \; y^* = (y/L)\sqrt{Re}, \; u^* = u/U_o,$$
$$v^* = (v/U_o)\sqrt{Re} \tag{11}$$
$$T^* = (T_w - T)/(T_w - T_e),$$
$$C^* = (C_w - C)/(C_w - C_e) \tag{12}$$

In eq. (11), U_o is the free-stream velocity, and Re is the Reynolds number based on the free-stream velocity and the characteristic length, L. Then the governing equations in dimensionless, stretched coordinate become

$$\frac{\partial u^*}{\partial x^*} + \frac{\partial v^*}{\partial y^*} = 0 \tag{13}$$

$$u^*\frac{\partial u^*}{\partial x^*} + v^*\frac{\partial u^*}{\partial y^*} - U^*\frac{\partial U^*}{\partial x^*} = \frac{\partial^2 U^*}{\partial y^{*2}} \tag{14}$$

$$u^*\frac{\partial T^*}{\partial x^*} + v^*\frac{\partial T^*}{\partial y^*} = \frac{1}{Pr}\frac{\partial^2 T^*}{\partial y^{*2}} \tag{15}$$

$$u^*\frac{\partial C^*}{\partial x^*} + v^*\frac{\partial C^*}{\partial y^*} = \frac{1}{Sc}\frac{\partial^2 C^*}{\partial y^{*2}} \tag{16}$$

where $Pr = C_p\mu/k$ is the Prandtl number, and $Sc = \nu/D$ is the Schmidt number. On going from eqs. (1)-(4) to eqs. (13)-(16), terms divided by the Reynolds number have been dropped out resulting in a boundary-layer approximation. The corresponding boundary conditions become:

$$u^*(x^*, 0) = v^*(x^*, 0) = 0 \tag{17}$$
$$T^*(x^*, 0) = C^*(x^*, 0) = 0 \tag{18}$$
$$u^*(x^*, \infty) = U^* \tag{19}$$
$$T^*(x^*, \infty) = C^*(x^*, \infty) = 1 \tag{20}$$

A Göertler-type transformation and finite difference approximation

Traditionally the numerical calculation of laminar boundary-layer equations has been performed in a similarity variable domain. In such a domain, the numerical grid approximately follows the growth of the boundary layer. The boundary layer over a 2-D bluff body is only locally similar. Therefore a certain modified form of similarity variable should be employed for this geometry. The one introduced here has been proved very useful in boundary-layer calcula-
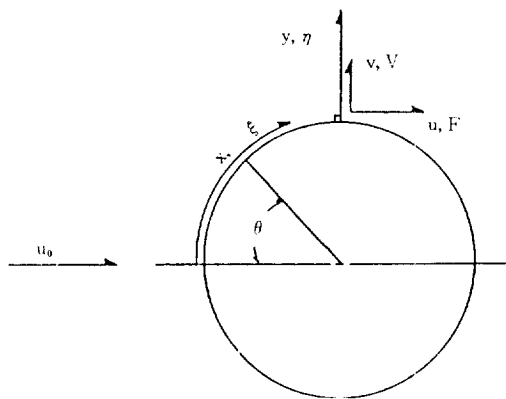
tions [9,10].

$$\xi = \int_0^{x^*} U^* \, dx^* \tag{21}$$

$$\eta = U^* y^* / \sqrt{2\xi} \tag{22}$$

A straightforward application of chain rule leads the following form of the governing equations:

$$2\xi F_\xi + F - V_\eta = 0 \tag{23}$$

$$F_{\eta\eta} + a_1 F_\eta + a_2 F + a_3 + a_4 F_\xi = 0 \tag{24}$$

$$T_{\eta\eta}^* + b_1 T_\eta^* + b_2 T^* + b_3 + b_4 T_\xi^* = 0 \tag{25}$$

$$C_{\eta\eta}^* + c_1 C_\eta^* + c_2 C^* + c_3 + c_4 C_\xi^* = 0 \tag{26}$$

where F is the normalized viscous velocity defined by

$$F = u^* / U^* \tag{27}$$

and

$$V = 2\xi \frac{\partial \eta}{\partial x^*} \frac{F}{U^*} + \frac{\sqrt{2\xi}}{U^*} v^* \tag{28}$$

The variable coefficients in eq. (24) are:

$$a_1 = -V \tag{29}$$

$$a_2 = -\beta F, \quad \beta = \frac{2\xi}{U^*} \frac{\partial U^*}{\partial \xi} \tag{30}$$

$$a_3 = \beta \tag{31}$$

$$a_4 = -2\xi F \tag{32}$$

Those in eq. (25) are:

$$b_1 = a_1 Pr \tag{33}$$

$$b_2 = b_3 = 0 \tag{34}$$

$$b_4 = a_4 Pr \tag{35}$$

Replacing Pr by Sc, these correspond to those in eq. (26). Equations (23) - (26) have been numerically integrated using a finite difference technique with a variable grid spacing.

An equal spacing was provided in streamwise direction, however the grid point spacing in normal direction was a geometric progression, i.e., the ratio of any two successive steps was a constant. Integration was first proceeded in the stagnation region along the normal direction, and then moved in downstream direction until the skin friction is vanished. This condition is a widely accepted criterion for steady separation.

Initial conditions to x=0 plane and the outer flow equations

As mentioned earlier, the boundary-layer calculations proceed by first providing the initial conditions to the front stagnation region and the outer flow equation. The boundary-layer flow is driven by the outer potential flow. The impinging flow on the narrow stagnation region of a circular cylinder is essentially a plane stagnation flow, and the well-known Hiemenz profiles [11] have been provided. These are:

$$G''' + GG'' - G'^2 + 1 = 0 \tag{36}$$

$$G(0) = G'(0) = 0, \quad G'(\infty) = 1 \tag{37}$$

where

$$f(y) = (\nu a)^{1/2} G(\hat{y}), \quad y = (\nu/a)^{1/2} \hat{y}, \quad u = xf',$$

$$v = -f \tag{38}$$

For further details, the reader is referred to Ref. (11).

Under the forced convection assumption, the temperature and concentration distributions near the stagnation point are readily obtained by substituting the velocity distribution into the governing equations i.e., into the thermal energy equation [eq. (3)] and the equation of continuity of diffusant [eq. (4)]. The results obtained upon substitution become

$$T_{yy} + fT_y Pr = 0 \tag{39}$$

$$T(0) = T_w, \quad T(\infty) = T_e \tag{40}$$

$$C_{yy} + fC_y Sc = 0 \tag{41}$$

$$C(0) = C_w, \quad C(\infty) = C_e \tag{42}$$

Equations (39) and (41) were first rewritten in stagnation coordinate defined in this section, and subsquently were solved with eq. (36). A package program (COLSYS) based on a collocation method was employed to solve these three boundary value problems numerically. The numerical solutions thereby obtained provided the initial conditions to x=0 plane in boundary-layer calculations.

A most important input to the boundary-layer calculation is the outer flow velocity distribution. The outer flow equation for a 2-D symmetric body with a stagnation point should be in the form of

$$U^* = A_1 x^* + A_3 x^{*3} + A_5 x^{*5} \tag{43}$$

where $x^* = 0$ is the mean stagnation point. In this equation the leading linear term is to ensure a stagnation flow, and terms of odd order are to guarantee the symmetry of the flow. Several outer flow equations including potential flow and experimentally determined outer flows are considered in the present calculations. Experimentally determined outer flow equation implies certain very important flow characteristics such as blockage effect, turbulence level and Reynolds number.
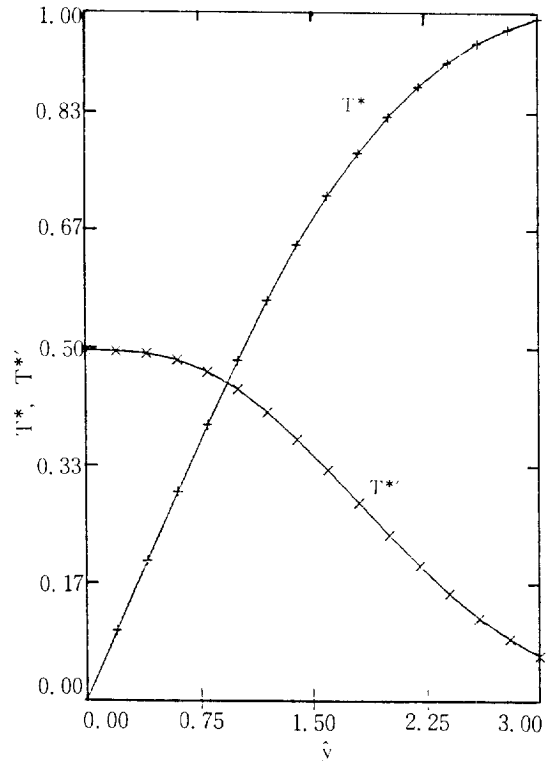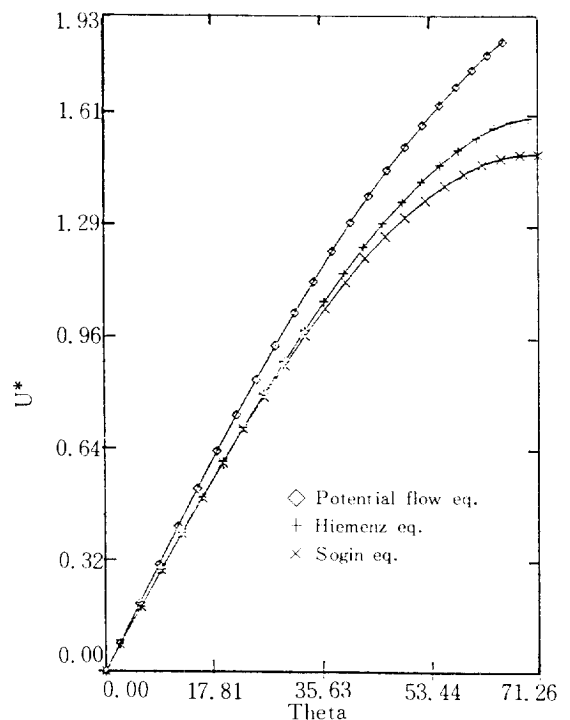
RESULTS AND DISCUSSION

Presently calculated numerical solution to eq. (36) is shown in Table 1. Shown in the same table is the numerical solution to the same equation by Höwarth [11] who made an improvement over Hiemenz original solution. The two results are identically the same. Temperature distribution around the stagnation point, i.e., the numerical solution to eq. (39) is displayed in

Table 1. The steady plane stagnation flow solution.

$\hat{y}$	G		G'		G''	
	present	Hö-warth	present	Hö-warth	present	Hö-warth
0.0	0.0	0.0	0.0	0.0	1.2259	1.2326
0.20000	0.02332	0.0233	0.22661	0.2266	1.03445	1.0345
0.40000	0.08806	0.0881	0.41416	0.4145	0.84633	0.8463
0.60000	0.18670	0.1867	0.56628	0.5663	0.67517	0.6752
0.80000	0.31242	0.3121	0.68594	0.6859	0.52513	0.5251
1.00000	0.45923	0.4529	0.77787	0.7779	0.39801	0.3980
1.20000	0.62203	0.6220	0.84667	0.8467	0.29378	0.2938
1.40000	0.79665	0.7967	0.89681	0.8968	0.21100	0.2110
1.60000	0.97978	0.9798	0.93235	0.9323	0.11735	0.1474
1.80000	1.16886	1.1689	0.95683	0.9568	0.09996	0.1000
2.00000	1.36197	1.3620	0.97322	0.9732	0.06583	0.0658
2.20000	1.55776	1.5578	0.98385	0.9839	0.04204	0.0420
2.40000	1.75525	1.7553	0.99055	0.9905	0.02602	0.0260
2.60000	1.95381	1.9538	0.99463	0.9946	0.01560	0.0156
2.80000	2.15300	2.1530	0.99705	0.9970	0.00905	0.0090
3.00000	2.35256	2.3526	0.99842	0.9984	0.00508	0.0051
3.20000	2.55233	2.5523	0.99919	0.9992	0.00275	0.0028
3.40000	2.75221	2.7522	0.99959	0.9996	0.00144	0.0014
3.60000	2.95215	2.9521	0.99980	0.9998	0.00073	0.0007
3.80000	3.15212	3.1521	0.99991	0.9999	0.00036	0.0004
4.00000	3.35211	3.3521	0.99996	1.0000	0.00017	0.0002
4.20000	3.55210	3.5521	0.99998	1.0000	0.00008	0.0001
4.40000	3.75210	3.7521	0.99999	1.0000	0.00003	0.0000
4.60000	3.95210	3.9521	1.00000	1.0000	0.00001	0.0000

Fig. 2. Stagnation region temperature distribution($T^{*'} = dT^*/d\hat{y}$).

Fig. 3. Outer flow velocity distributions.

Fig. 2. This together with the velocity profile shows an asymptotic behavior which is a most important boundary-layer characteristic. Though not presented here, numerical solution to eq. (41), i.e., concentration distribution near the point of stagnation, also showed an asymptotic tendency. These three stagnation profiles were then recast in boundary-layer coordinate, and fed to the boundary-layer code to initialize the boundary-layer calculations.

With the stagnation region solutions, the boundary-layer calculations proceed by providing the outer flow conditions in terms of outer flow velocity distribution. Outer flow velocity distributions tested in the present study are plotted in Fig. 3. In the figure, potential flow corresponds to $A_1 = 2.0$, $A_3 = 0.333$ $A_5 = 0.016$, and those for Hiemenz profile are $A_1 = 1.814$, $A_2 = 0.271$, $A_3 = 0.047$, and the Sogin profile corresponds to $A_1 = 1.82$, $A_3 = 0.400$, $A_5 = 0.000$. The latter two profiles

are polynomial curve fit to the experimental data in Ref. (2), and Ref. (12), respectively. The skin friction distributions corresponding to the outer flows in Fig. 3 are given in Fig. 4. In both figures, the deviation among the three types of outer flow is notable as the point of separation is neared. Potential flow obviously designates no separation in contrast to a laminar separation at about 82° from the front stagnation point for a wide range of Reynolds number i.e., in the sub-critical region. Actual separation point is however very sensitive to the external flow conditions such as free-stream turbulence level and blockage. With about one percent free-stream turbulence, for example, the point of separation is delayed by 5-7°[13,14].

Presently predicted rate of heat transfer corresponding to the outer flows mentioned is shown in Fig. 5. A notable difference in heat transfer between potential flow and experimental outer flows is demonstrated. Present method of prediction of heat transfer is now compared with many other predictions in Fig. 6. The details of other prediction methods are found in Ref. (2). The outer flow equation is common for all of the methods including the present one, i.e., the Hiemenz outer flow which is a curve fit of experimental data by Schmidt and Wenner [2]. Spalding and Pun [2] rated over fifteen prediction methods by comparing each of them with Frössling's exact solution up to 45° from the
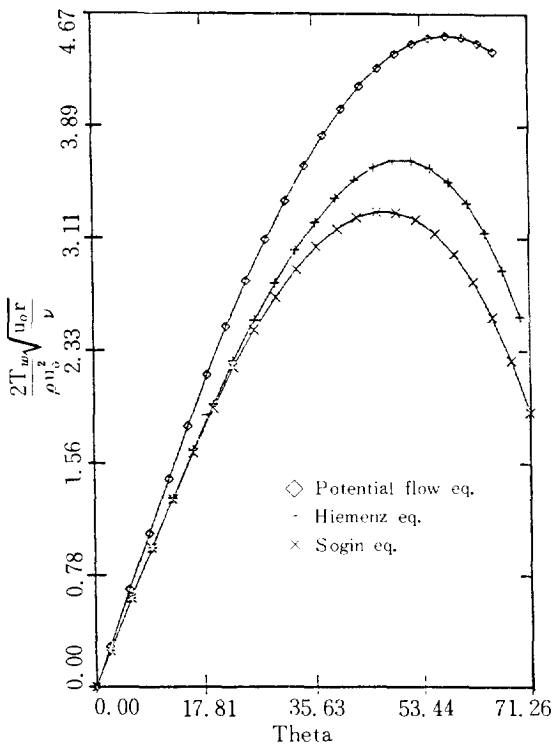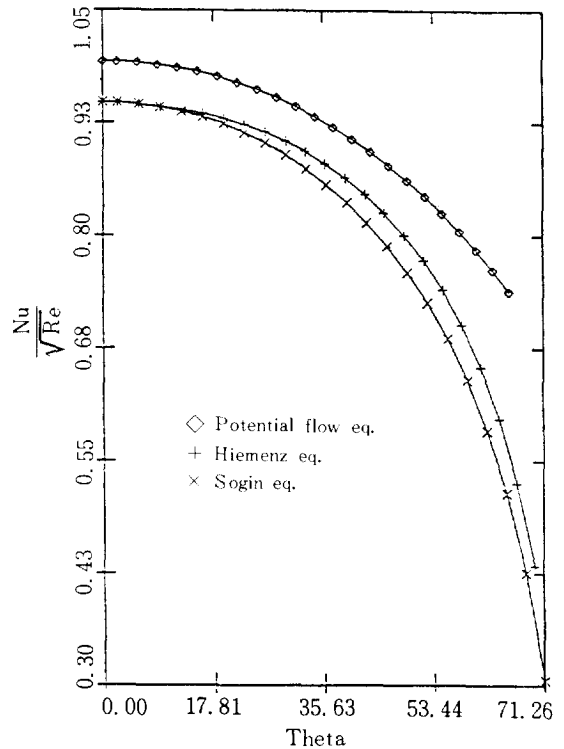

Fig. 5. **Local rate of heat transfer(Pr = 0. 7).**
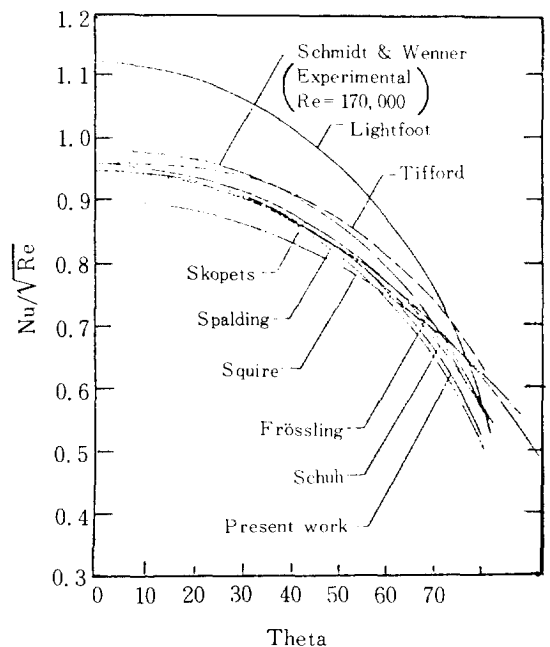

Fig. 4. **Skin friction distributions.**

Fig. 6. **Local rate of heat transfer predicted by many different methods(Pr = 0. 7).**
Names represent methods in Ref. [2].

stagnation point and the experimental data by Schmidt and Wenner beyond this point. The present results are very close to the one by Spalding and Pun, however, underestimate compared to the experimental data. The same tendency is seen for other predictions which are ranked high by Spalding and Pun. At least three possible reasons may be considered for this common discripancy between the theoretical prediction and experimental data: the constant property assumption, the free-stream turbulence effect and the unsteadiness effect due to the natural shedding. The constant property assumption is a premise of forced convection and will certainly be in part responsible for underestimation. The effect of natural shedding on local rate of heat transfer is being examined in detail and will be reported later. The effect of free-stream turbulence level on heat transfer has in the past been carefully studied by many investigators and well documented in Ref. (15). It is nowadays well understood that the free-stream turbulence enhances the heat transfer, for example, local rate of heat transfer is approximately doubled by one percent increase in turbulence level at low turbulence level.

Finally the local rate of mass transfer is shown in Fig. 7. The case interested here is the sublimation of solid naphthalene into air [12]. The experimental conditions were such that a forced convection was valid i.e., the experiment was done at Re = 122,000 with the naphthalene concentration less than 0.1% of air in air stream. It is not difficult to show that the characteristic mass transfer group in this case is the Sh/ √Re (Sh = mass transfer coeff × cylinder diameter/D = Sherwood number), and this is obtained by

$$\mathrm{Sh}/\sqrt{\mathrm{Re}} = 1.4142 \, \frac{\mathrm{U}^*}{\sqrt{2\xi}} \, \frac{\partial C^*}{\partial \eta} \Big)_{wall} \qquad (44)$$
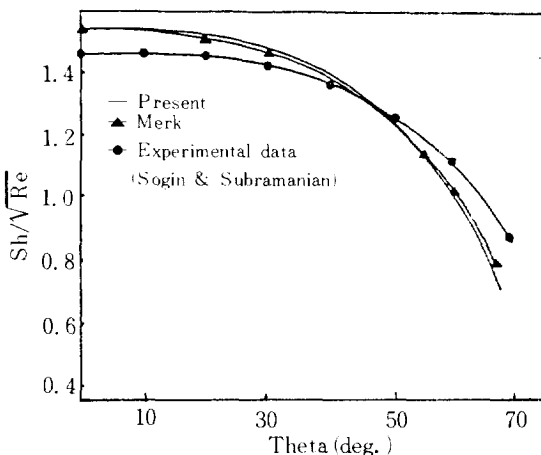

Fig. 7. Local rate of mass transfer.
  Sublimation of naphthalene into air, Sc = 2.5

The predicted mass transfer overestimates up to about 50° from the front stagnation point, and underestimates beyond this point compared to the experimental data by Sogin and Subramanian [12]. Also shown in the same figure is theoretical prediction by these authors using Merk's method. The two theoretical predictions show similar tendency. The outer flow equation used in both predictions was an experimentally determined one by Sogin and Sabramanian [12], and denoted by Sogin equation in Fig. 3. The reason why the theoretical prediction of local mass transfer near the stagnation point is higher than the experimental data is not clear. Probably, a more correct outer flow measurement will give a clue to this question.

CONCLUSION

An exact numerical solution to the two-dimensional laminar boundary-layer equations of continuity, momentum, heat and mass transfer has been numerically solved by the method of finite difference. The solutions to the thermal energy equation and convective mass transfer equation have for the first time been solved by this method under forced convection. Exact numerical solutions for the stagnation region temperature and concentration distributions also provided correct initial conditions to the boundary-layer calculation. Essentially the outer flow velocity distribution dictated the rate of transport process across the boundary-layer.

Results obtained in the present work were comparable with experimental data available, and certainly made an improvement over past analytical approximation. This was especially the case for heat transfer. Predicted local rate of mass transfer, however was not in a good agreement with the experimental data available. This may probably, at least in part, due to the outer flow equation employed in the present calculation. By providing a carefully measured outer flow velocity distribution, a better agreement with the experimental data is expected.

ACKNOWLEDGEMENT

NOMENCLATURE

a   : Constant in stagnation region velocity
A_i : Coefficients in outer flow equation
C   : Concentration
C_P : Specific heat at constant pressure
D   : Binary diffusity
f   : Stagnation function defined by eq. (38)

F : Normalized velocity defined by eq. (27)
G : Stagnation function defined by eq. (38)
L : Characteristic length
T : Temperature
u : Streamwise velocity, dimensional
U : Outer flow velocity, dimensional
v : Normal velocity, dimensional
V : Normal velocity defined by eq. (28)
x : Streamwise coordinate, dimensional
y : Normal coordinate, dimensional
$\dot{y}$: Stagnation region normal coordinate defined by eq. (38)

Subscripts and Superscripts
w : Condition at wall
e : Condition at boundary-layer edge
* : Dimensionless quantity defined by eqs. (11) and (12)

Dimensionless Groups
Re : Reynolds number = $LU_o \rho / \mu$ (U_o = free-stream velocity)
Sc : Schmidt number = ν / D
Sh : Sherwood number = bL/D (b = mass transfer coefficient)
Pr : Prandtl number = $C_F \mu / k$ (k = thermal conductivity)

Greek Letters
α : Thermal diffusity
η : Normal coordinate defined by eq. (22)
μ : Viscosity
ν : Kinematic viscosity
ξ : Streamwise coordinate defined by eq. (21)
ρ : Density
τ_w : Wall shear stress
θ : Angle measured from the front stagnation point

REFERENCES

1. Winding, C.C. and Cheney, A.J.: *Ind. Eng. Chem.*, **40**, 1087 (1948).
2. Spalding, D.B. and Pun, W.M.: *Int'l. J. Heat & Mass Trans.*, **5**, 239 (1962).
3. Zukauskas, A.: "Advances in Heat Transfer", 8, Academic Press, New York, NY (1972).
4. Frossling, N.: NACA TM 1433, 1940.
5. Chao, B.T.: *Int'l. J. Heat & Mass Trans.*, **15**, 907 (1972).
6. Sano, T.: J. Heat Trans., Trans. ASME, **3**, 100 (1978).
7. Krall, K.M. and Eckert, E.R.: Heat Transfer 1970, 3, FC7. 5(1970).
8. Bird, R.B., Stewart, W.E. and Lightfoot, E.N.: "Transport Phenomena", Wiley, New York, NY (1960).
9. Telionis, D.P.: "Unsteady Viscous Flow", Springer, New York, NY (1981).
10. Telionis, D.P., Tsahalis, D.T. and Werle, M.J.: *Physics of Fluid*, **16**, 968 (1973).
11. Schlichting, H.: "Boundary-Layer Theory", 7th ed., McGraw-Hill, New York, NY (1079).
12. Sogin, H.H. and Sabaramanian, V.S.: *J. Heat Trans.*, *Trans.* ASME, 483 (1961).
13. Borell, G., Kim, B.K., Ekhaml, W., Diller, T.E. and Telionis, D.P.: "Pressure and Heat Transfer Measurement", Presented at 1984 ASME Fluid Engineering Conference, New Orleans, (1984).
14. Kim, B.K.: Ph D Dissertation, Virginia Polytechnic Institute and State Univ. (Dec. 1984), Blacksburg, Virginia, U.S.A.
15. Saxena, U.C. and Laird, A.D.: *J. Heat Trans.*, *Trans.* ASME, **3**, 100 (1978).